Cold Regions Science and Technology 157 (2019) 163–170

Contents lists available at ScienceDirect

Cold Regions Science and Technology

journal homepage: www.elsevier.com/locate/coldregions

Quantifying snow drift on Arctic structures: A case study at Summit, Greenland, using UAV-based structure-from-motion photogrammetry

Robert L. Hawley*, Joanna D. Millstein

Department of Earth Sciences, Dartmouth College, Hanover, NH 03755, USA

ARTICLE INFO

Keywords:
Photogrammetry
Drifting
Snow
UAV
SfM
Greenland

ABSTRACT

Designing a building for polar stations involves countless cost-benefit trade-offs. One critical decision for planners is whether to elevate structures or place them on the snow surface. For planners wishing to minimize the impact of drifting, elevated structures are generally more desirable, with the tradeoff of added construction cost. Surface-based structures are less expensive to construct, but accumulate drift more rapidly than their elevated counterparts, thus incurring an added recurring expense of snow removal. To estimate this added cost, we quantified the volume of snow drifted on several structures at Summit, Greenland, using structure-from-motion photogrammetry from a small UAV. We find that while the elevated "Bighouse" accumulated negligible drift, the surface-based "Greenhouse" accumulated $4862 \pm 444\,\mathrm{m}^3$ of snow. We then use estimates of equipment efficiency at snow removal coupled with equipment operating cost to determine the time and cost of snow removal (69 ± 6 h for the Greenhouse). Finally, we analyze a 10-year record of winds from Summit, and estimate the total amount of snow drifted on the structures in any given year. We estimate that the Greenhouse at Summit accumulates an average of $11{,}702\,\mathrm{m}^3$ of snow per year, and that clearing that snow costs an average of $41,000 per year. The expense of snow removal for surface-based structures should be factored into the total lifetime cost of the building, making elevated structures much more cost-competitive than they may initially appear.

1. Introduction

When the wind blows in the Arctic, anything sitting on the snow surface can quickly be buried in drifting snow. Wind speeds as low as 6 m/s (13 MPH) can entrain and move snow (Tabler, 1994). Once in motion, drifting snow settles when the air carrying it is blocked by an obstacle, such as a building or vehicle. This "Drifting in" is a well-known inconvenience at polar camps and stations. For occupied structures located on the snow surface, drifting can block egress from the building, leading to hazardous conditions (Haehnel and Weatherly, 2014). Clearing the drift from these structures can become time-consuming and expensive. Elevating structures above the snow surface effectively eliminates drift (Kwok et al., 1992), clearly making it desirable, but raises the cost of construction significantly, leading to a trade-off for planners, who need data on which to base their decisions. Recent redevelopment plans at Summit Station have prioritized elevated structures in an effort to reduce maintenance costs and increase station sustainability. It is therefore desirable to quantify and predict the amount of snow drifted by any given structure, and estimate subsequent snow removal costs, for both logistical and financial planning.

Here, we quantify the volume of drifted snow around several structures at Summit Station, Greenland. Structures at Summit perennially drift in and are cleared by crews with heavy equipment. We generated a digital elevation model (DEM) of the station, using Structure-from-motion (SfM) photogrammetry on images acquired using a small (2 m wingspan) fixed-wing unmanned aerial vehicle (UAV). Using this DEM, we calculated the drift volume around structures, and relate the volume to the amount of heavy-equipment time needed to clear the structures. We use a 10-year meteorology record and established wind/drift relationships to determine the amount of snow expected to drift on a structure in any given year, and thus the total annual cost of snow removal for surface-based structures. Finally, we illustrate the compounded effect of 26 years of drifting on the whole Summit Station area using a DEM generated from satellite imagery.

2. Background

2.1. Snow drift modeling

The impact of drifting snow on structures has been of interest since

* Corresponding author.
E-mail address: robert.l.hawley@dartmouth.edu (R.L. Hawley).

https://doi.org/10.1016/j.coldregions.2018.10.007
Received 2 April 2018; Received in revised form 15 October 2018; Accepted 18 October 2018
Available online 20 October 2018
0165-232X/

permanent structures were first placed on a snow surface. Many studies have measured and modeled snow drift, attempting to quantify its effect on buildings. The rate of snow mass transport is very sensitive to wind speed (Kind, 1986). Snow is transported by wind in three dominant modes: 1) Suspension of snow particles in air, 2) Saltation, in which particles are suspended temporarily as they bounce along the surface, and 3) Traction, in which snow particle are dragged along the surface. Of these, saltation is the dominant mode of mass transport in snow drifting (Pomeroy and Gray, 1990). More recently, advanced physically-based and Computational Fluid Dynamics (CFD) models of snow drifting have been developed (Gauer, 2001; Liston et al., 2007; Tominaga et al., 2011).

Many of these higher-complexity 3-D models have been validated in the field. Schneiderbauer and Prokop (2011) successfully simulated the evolving interaction between terrain and snow deposition at a test site in the Austrian Alps. Vionnet et al. (2014) matched blowing fluxes as measured by snow particle counters, and showed correct erosion and deposition of snow on rough terrain. These models show excellent fidelity for capturing complex flow around and over topographic features.

2.2. Snow drifting- measurements

Many investigators have made measurements of drifting under both laboratory and field conditions. Tominaga et al. (2013) measured saltation rates using Particle Image Velocimetry in a laboratory wind tunnel, concluding that snow particle velocities under saltation are 40% lower than wind velocities. In the field, Jaedicke (2001) used an acoustic instrument (FlowCapt) to measure drifting snow via the impacts of snow particles on the instrument. Jaedicke (2001) concluded that the bulk of snow transport happens in the bottom-most 0.5 m of the wind column, by up to a factor of 10 in mass flux. Schön et al. (2015) used terrestrial laser scanning (TLS) to help improve estimates of a terrain parameter to determine the likelihood of erosion or deposition, which is dependent on terrain morphology.

In populated regions, snow fences are constructed to mitigate the effect of drifts on roads, slopes, and structures. Prokop and Procter (2016) used TLS to measure snow drift patterns around snow fences. They made scans before and after major drift events, enabling them to determine the total volume of additional drifting from a given event. This information, combined with wind field modeling, allowed them to identify alternative configurations for the snow fences. Basnet et al. (2016) demonstrated the use of close-range photogrammetry (CRP; closely related to traditional photogrammetric techniques, as distinct from Structure-from-Motion) to measure and monitor drifting patterns on a snow fence. They illustrated an automated approach that overcomes traditional survey methods, which are expensive in either time or capital equipment cost.

In Greenland, Haehnel and Bigl (2016) measured drifting in the central area of Summit Station using repeat Global Positioning Service (GPS) surveys to construct DEMs. Differencing two DEMs separated in time revealed surface changes related to drifting, accumulation, and mitigation. Analyzing wind records and using snow transport theory, they found that most drifting at Summit is in winter.

2.3. Measuring snow drifting and topography with SfM

Traditional photogrammetry, even using modern digital imagery, requires that the relationship between camera positions is known. Structure-from-Motion (SfM) is a technique introduced by Koenderink and Van Doorn (1991), in which both the geometry of coincident points in two images and the unknown camera positions from which the images were taken can be determined simultaneously. While first conceptualized for use in computer vision, the idea is well-suited to the problem of low-cost photogrammetry. Snavely et al. (2008) further developed the application to photography, and provide an excellent overview of the SfM process, as applied to reconstructing scene geometries from overlapping images where nothing about camera position is known.

Westoby et al. (2012) and Fonstad et al. (2012) publicized SfM as a useful tool in the geosciences, with specific applications to hillslope and fluvial geomorphology. Using a small UAV for an airborne survey, Hugenholtz et al. (2013) showed that the resulting terrain model from SfM had comparable accuracy to that achievable by lidar. The cryopshere community has more recently made use of SfM as well (eg. Piermattei et al., 2015; Ryan et al., 2015). Of particular interest in our study, Nolan et al. (2015) showed that SfM performs well on snow, in spite of a relative lack of features for image matching.

Multiple studies have been conducted with the specific target of determining snow depth. Cimoli et al. (2017) evaluated the capability of UAV-based SfM for snow-depth mapping in the Arctic. Using two sites in Svalbard and 4 in Greenland (on the ice-free coast, so mapping seasonal snow only), they created Snow DEMs (SDEMs) and Terrestrial DEMs (TDEMs). The difference between SDEM and TDEM is the snow depth at the time of the SDEM data acquisition. Bühler et al. (2016) conducted several tests in the Swiss Alps using an octocopter-mounted camera system, to map snow depth variations in both sheltered valley and exposed alpine terrain. Similar to Cimoli et al. (2017), they subtracted snow-free DEMs from snow-covered DEMs to determine snow depth.

Both of the aforementioned studies used marked Ground Control Points (GCPs), surveyed with GPS, to georectify the products of the aerial surveys. Alternative approaches have also been tested. Bernard et al. (2017) used the on-board GPS from the UAS in positioning the DEM for a snow-distribution study. Since the on-board GPS was navigation-grade (as opposed to survey-grade), some distortion was reported. Miziński and Niedzielski (2017) introduced a new method by which the use of GCPs could be eliminated for determining snow depth. Also using a difference-of-DEM approach, Miziński and Niedzielski (2017) co-register the two point-clouds using an iterative closest point approach, relying on features that can be identified in both point-clouds, such as trees that stand above the snowpack.

2.4. Impact on buildings and mitigation

When drifting snow encounters a building, the building impedes air motion, slowing the air and allowing the snow to be deposited. Smedley et al. (1993) used a wind-tunnel and a 1/100 scale model to simulate drifting on Davis Station, Antarctica, and experiment with mitigation strategies that did not involve lifting the building. Smedley et al. (1993) attached “spoilers” to the downwind edge of the structure in an attempt to affect the drift volume and shape. Of the two types of attachments used, one was abandoned before the test was complete as it actually increased drift. The second did not decrease drift volume, but solved the problem of egress from the building by maintaining the drift roughly one building-height downwind of the building. Of note, this changed nothing on the upwind side of the building.

Kwok et al. (1992) used similar wind-tunnel experiments to investigate the effect of elevating structures, and to determine the interaction between adjacent structures. Importantly, Kwok et al. (1992) found that the height of elevation is critical; by elevating the structure 32% of its own height above the surface, the total volume of drifted snow remains the same as a surface-based building (though it is detached from the leeward wall of the building, a significant improvement). By raising the building to 54% of its own height, the drift volume was decreased by a factor of 5. Kwok et al. (1992) did not investigate higher elevations such as 75% or 100% of the height of the structure, which are not uncommon in modern elevated structures. For example, the largest hard-sided structure at Summit, the Bighouse, is elevated 100% of its height above the snow and creates minimal drifting (see Section 5.1 and Fig. 8).

Orienting the long axis of a surface-based building parallel to the prevailing snow transport direction can mitigate drifting. Haehnel and Bigl (2016) found that snow transport at Summit has not one predominant direction but two, and they are orthogonal. Thus there is no optimal building orientation.

3. Methods

3.1. Field area

Summit Station (72 °N, 38 °W, 3250 m.a.s.l.) is at the location of the Greenland Ice Sheet Project II (GISP-II) ice core. Summit has been occupied seasonally since 1989. Several experimental year-round occupations of the station began in the boreal winter of 1997–98, and Summit has operated as a year-round facility since 2003. The station is staffed through the winter by a crew of 4–5, but often hosts larger populations for ‘campaign’ science in the summer. The typical summer population at Summit is 10–20 but can grow to as many as 60.

The first hard-sided structure, known as the ‘Bighouse’, was elevated above the snow not long after the camp was established. For several years it was the only hard-sided building on site, and other temporary soft-sided structures were erected seasonally to suit the needs of the camp. In the spring of 1997, to accommodate the winter occupation of the camp, a new laboratory and living space was constructed, known as the ‘Greenhouse’. This building was not elevated but placed on the snow surface. At the same time, the first soft-sided ‘garage’ was erected, and Summit has had a large surface-based tent for vehicle maintenance ever since. The existing garage at the time of our survey, the ‘Science and Operations Barn’ (SOB) was erected on a berm (an artificial ridge elevated above grade level, constructed with heavy equipment) in the summer of 2010. These buildings are between 10 and 30 m on a side. Other, smaller buildings have been brought to or built at Summit over the years, most of them placed on the snow surface. More recent development at Summit has focused on raised buildings.

3.2. Aerial images

To acquire high-resolution aerial imagery, we flew a small (~2 m wingspan) fixed-wing unmanned aerial vehicle (UAV; QUEST 300) over the field site on 8 June 2015. The QUEST 300 is launched by hand with a catapult assist (Fig. 1). Once airborne, the UAV is controlled by autopilot and follows waypoints along a pre-programmed flight path. Ground operators can monitor the position and status of the UAV via data telemetered to a control laptop, and can modify the flight path in real-time or take over manual control. Landing is via remote-triggered parachute, reducing the chances of damage. Our UAV carried a Sony NEX-7 digital camera in an active gimbal mount, ensuring stability of the photo platform by compensating for aircraft roll. The camera was triggered at 1 s intervals by the autopilot during the ~45 min flight, yielding a set of highly-overlapping digital photos of the field area.

Fig. 1. Launch of our QUEST 300 UAV. The catapult launch line extends 20 m to the left of the photo and is anchored in the snow. Ground control is via laptop computer with telemetry. Photo: Stephanie Wissel.

3.3. Ground-control point survey with DGPS

For scaling of the 3-dimensional reconstruction described in Section 3.4, we established 8 ground-control points within the survey area. We surveyed key identifiable points on the ground using a Trimble NETR9 survey-grade receiver with a Zephyr Geodetic antenna. At each point we collected 1 Hz GPS data for ~10 min, and measured the height of the antenna. Using reference station data from the continuously-recording base-station at Summit, we post-processed the GPS data using double-differencing techniques (RTKLib: www.rtklib.com), resulting in cm-scale solutions for both position and elevation. We used the final post-processed ground-control point positions both in constructing our high-resolution DEM, and also to adjust the absolute elevation of our WorldView DEM (Section 4.2).

3.4. High-resolution DEM with SfM

For our survey, we used Agisoft Photoscan Pro Version 1.1.6 software to build our digital elevation model of Summit Station and the surrounding region, using 392 photos from our aerial survey. After initial image feature matching and aligning, we used our high-precision DGPS ground-control-points (Section 3.3) to assist alignment and to georeference the DEM. Fig. 2 shows a subset of the final 3-d reconstruction, showing one of the buried structures.

3.5. Uncertainty in the resulting DEMs

Quantifying the uncertainty associated with a DEM resulting from SfM poses a logistical challenge. The ideal way to quantify uncertainty in this process is to collect, along with the GCPs for calibrating and georeferencing the DEM, additional validation points surveyed identically to the GCPs and identifiable in the SfM imagery. The challenge herein is the additional time associated with collecting these validation measurements. Since we had limited time in which to collect survey measurements, we chose to use all of our measurements as GCPs to create the best DEM possible. We evaluate the uncertainty of our final product based on a review of the available literature on accuracy of SfM DEMs in unfavorable conditions and over snow.

In an excellent example of a “gold standard” study, Jaud et al. (2016) used an octocopter in a rugged region of the island of Reunion specifically to asses the accuracy of DEMs produced by SfM. They used

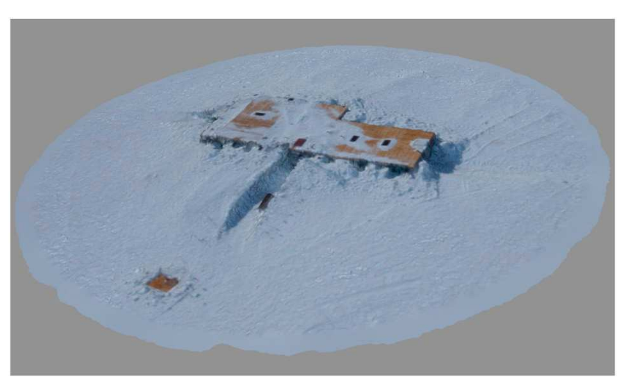

Fig. 2. Prospective view of the Summit Greenhouse; color imagery draped over the SfM-derived DEM. Note that the drifting at this point in time is near equilibrium.

12 GCPs to construct the DEM and also collected the GPS positions for 9 validation points, not used in the DEM construction. The differences between the elevations of these 9 reference points as computed in the SfM DEM and as measured by GPS then amounts to an excellent assessment of the achievable absolute accuracy of a DEM from SfM. In the processing scenario most closely related to our situation the vertical root-mean-squared error (RMSE) reported by Jaud et al. (2016) was 0.124 m.

To address the capability of SfM on snow, which has far fewer features with which to match points between photos, two studies are of interest. In both studies the aircraft (one manned, one UAS) had survey-grade GPS onboard, eliminating the need for GCPs for DEM calibration. Using a manned aircraft, Nolan et al. (2015) found mean elevation offsets of 0.13 m. Harder et al. (2016) used a UAV with GPS and a real time kinematic (RTK) link to improve camera position accuracy. The RMSE reported for an alpine mountain surface in this study was 0.085 m.

Many studies are mainly concerned with snow depth accuracy, rather than absolute elevation accuracy. Thus it is the difference between two SfM DEMs that is important. If we take the snow-free DEM to be correct, the RMSE of reported snow depths can be related to the RMSE of the snow-covered DEM. Cimoli et al. (2017) evaluated the SfM-derived snow depths by using an avalanche probe to manually determine snow depth at each GCP, to compare directly with the retrieved snow depth. The resulting estimated error averaged 0.10 m over 6 independent surveys. Cimoli et al. (2017) note that this could be an optimistic estimate, as the validation points were close to the GCPs, and thus would be where the DEM reconstruction was best. Jaud et al. (2016) did not suffer this problem. Using the same validation technique for snow depth, some of the RMSE values reported by Bühler et al. (2016) are greater than those of others (~0.3 m maximum), but these are likely due to the complicating factor of vegetation on the process; the snow-free DEM surface is higher than the actual ground surface due to the vegetation, which presses down towards the ground under the weight of the overlying snow. On more sparsely-vegetated areas, Bühler et al. (2016) found RMSE for snow depth between 0.07 and 0.15 m.

Taking the largest of these reasonable RMSE estimates, we assume our DEM reproduces the actual snow surface at Summit with an RMSE of no more than 0.15 m. Since this is an RMSE rather than a bias, propagate this uncertainty by evaluating the volumes in question if the surface were 0.075 m lower than reported (the minimum volume) or if it were 0.075 m higher than reported (the maximum volume).

4. Results

4.1. Quantification of drift volume

We investigated three specific subsections of our survey area to quantify three different types of drifting challenges. The first and simplest case was a simple mound of snow to the north of Summit (labeled 'a' in Fig. 3). This temporary mound was built by equipment operators in the previous season while moving snow away from the station, and served as storage until the snow could be pushed farther from Summit. To quantify the volume of this mound (hereafter the 'deficit pile') we define a base elevation as the original surface elevation at the location of the pile, noting that this horizontal plane may differ from local topography after removal. The volume of the pile is then simply the volume integral of the surface elevation of the pile with the base elevation subtracted. This process is illustrated schematically in Fig. 4.

A slightly more complicated scenario is presented in excavating the SOB. Since Summit naturally accumulates roughly 0.65 m of snow each year (Dibb and Fahnestock, 2004), surface structures will eventually become buried below grade, even in absence of drifting. Though the SOB was initially constructed on a berm above grade, its base was significantly below grade by the time of our survey. Thus to maintain access to the structure, equipment operators must create a bowl-shaped depression around the building. In this case, we measure not the volume of existing snow but the volume that must have been removed to create the bowl. To do this we define grade level by connecting the surface on either side of the bowl with a plane, and determine the volume between grade level and the floor of the bowl at the time of the survey. Note that we remove the volume of the building and the heavy equipment parked adjacent to the building for this calculation. A schematic illustrating this process can be see in Fig. 5.

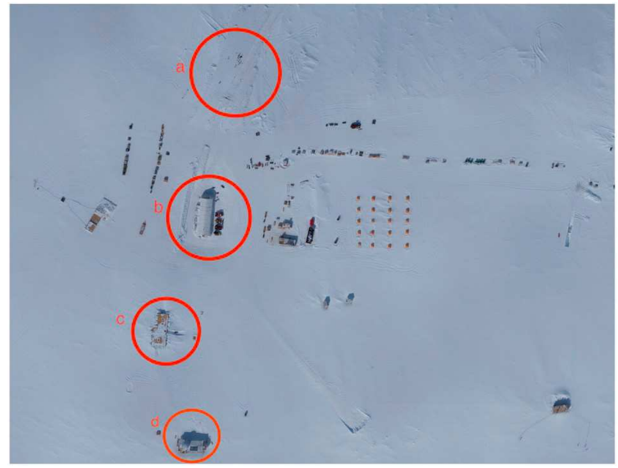

Fig. 3. A portion of our final orthophoto mosaic of Summit, showing several of the main structures. The grid of 20 small yellow squares near the center of the image is 'tent city' accommodation for summer population. The 'Big house' is near the bottom of the image. Circles indicate a pile of snow in the process of being moved off station (the 'deficit pile'; a), the Science Operations Barn (SOB; b), the Greenhouse (c), and the Bighouse (d).

Finally, we address the case of a building that was placed on a berm, yet still becomes drifted close to the roof line. For this case we use the Greenhouse. To determine the snow removal required to clear this structure, we establish a base level which is even with the original berm on which the structure was placed. The remainder is similar to the procedure we used when calculating the volume of the 'deficit pile', with the exception that we masked the building itself from the analysis. The schematic illustrating this case is in Fig. 6.

4.2. Summit area from PGC DEMs

While the general accumulation of snow in the Summit region averages 0.65 m per year (Dibb and Fahnestock, 2004), over the nearly thirty years Summit has been established drifting around structures and cargo has caused a higher effective accumulation. Since structures are periodically moved to new locations at or above the new grade level, the ultimate effect is for the local area of Summit to rise above the surrounding grade. This effect is subtle and not obvious to the eye at Summit, but can be clearly seen on a larger-scale DEM of the area. To examine the more broad aspects of drifting at Summit, we used a DEM created by the Polar Geospatial Center from DigitalGlobe, Inc. imagery. Although restoring the original grade of the ice sheet in this region would be cost-prohibitive, the total volume added to the Summit area to date is still of interest. We follow a similar procedure to that used above for calculating drifting around buildings, but this time establish the regional grade around summit as a base level. We integrate the volume between the existing surface and the base level to determine the volume of additional accumulation around the Summit area. A schematic for this operation is shown in Fig. 7.

4.3. Final volumes

The final volumes determined for the four regions outlined in

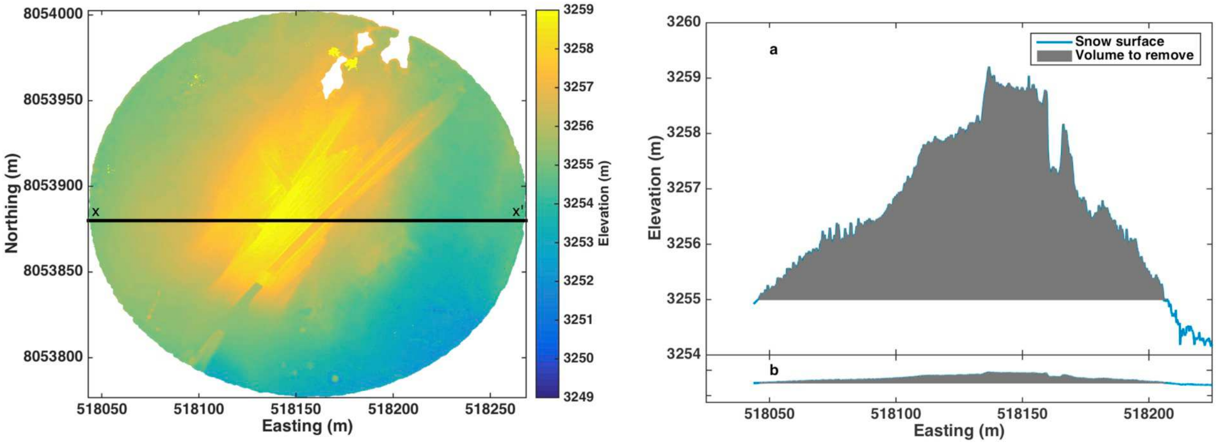

Fig. 4. Determining the volume of the 'deficit pile'. Left: map-view showing elevations surrounding the pile, and cross section x-x'. Right, panel a) shows the snow surface along the transect x-x', the base level, and the volume of snow to be removed. Note vertical exaggeration. Panel b) shows the same view with no vertical exaggeration.

Sections 4.1 and 4.2 are summarized in Table 1. We find the two structures to have similar "Volume to clear" the structure, in spite of the size difference between the two buildings, and the difference in base level. This is likely an artifact of how we define the "volume to clear". For the SOB, we took as the volume to clear the bowl in which the SOB sits. In reality, drift will accumulate well above that level if left untended, ultimately to the top of the structure as is the case with the Greenhouse. Since we did not have any actual drifted snow surface with which to work (ie the bowl is indeed cleared out and maintained throughout most of the year), we chose to use the volume of the bowl rather than potential drift volume. The "deficit pile" is, not surprisingly, substantially larger as it contains the snow cleared away from multiple structures.

4.4. Equipment hours

In addition to computing volumes of snow, we estimated the amount of equipment time required for its removal. For the Caterpillar bulldozers at Summit, we estimate a pushing efficiency of $70\,\mathrm{m^3 hr^{-1}}$ (Haehnel and Weatherly, 2014). Table 1 lists the number of equipment hours estimated to clear each of the sub-volumes we have calculated. Note that clearing the fully-drifted Greenhouse takes roughly an entire 6-day work week of full-time equipment usage, and that to move the entire "Summit bulge" would take roughly 5 years of full-time, year-round effort.

5. Discussion

5.1. Counterpoint: an elevated building

In addition to the surface-based buildings in our survey at Summit, our survey also included the area around the 'Bighouse', the original hard-sided structure, which is elevated and raised periodically. At the time of our survey it was elevated approximately a full building-height above the snow surface, well above the range analyzed by Kwok et al. (1992). As a counterpoint to the drift analysis of the surface-based buildings, we investigated the surface around the Bighouse for evidence of drifting. An overview and cross-section of the area around the Bighouse can be seen in Fig. 8. Little to no evidence of drifting is apparent in the profile, which slopes upward towards the berm on which the Greenhouse sits directly to the north (Fig. 3). As is often seen in elevated structures, accelerated winds under the structure create a 'scour' feature underneath the building, which is clearly visible on the cross section. It is important to note that previous studies (Haehnel and Bigl, 2016) found a small amount of deposition downwind of the Bighouse from the winter of 2012–2013, though the reason for this difference remains unclear.

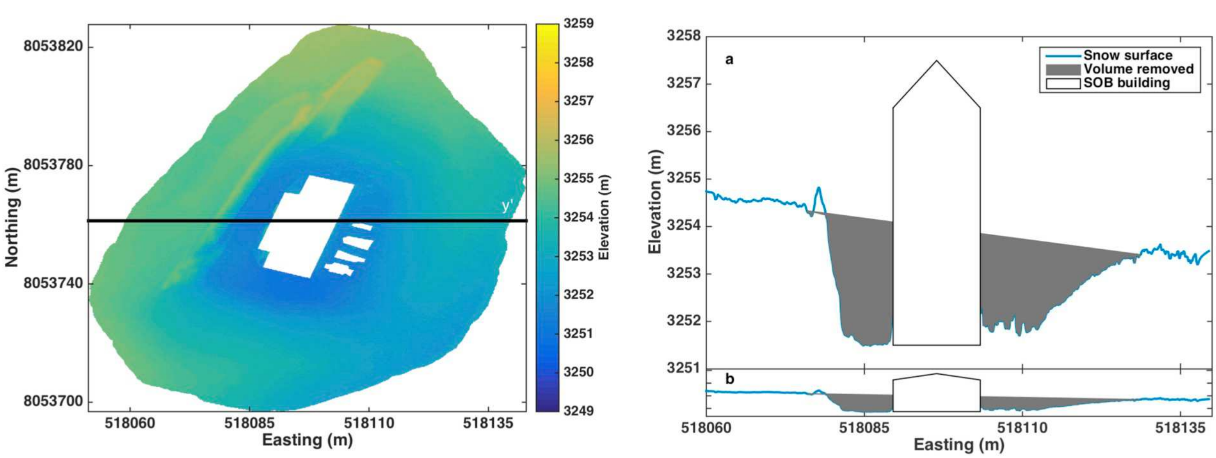

Fig. 5. Determining the volume of snow removed to maintain access to the SOB. Left: map-view showing elevations surrounding the SOB (note the structure itself and the equipment parked next to it are masked), and cross section y-y'. Right, panel a) shows the snow surface along the transect y-y', the grade level, and the volume of snow to be removed. Note vertical exaggeration. Panel b) shows the same view with no vertical exaggeration.

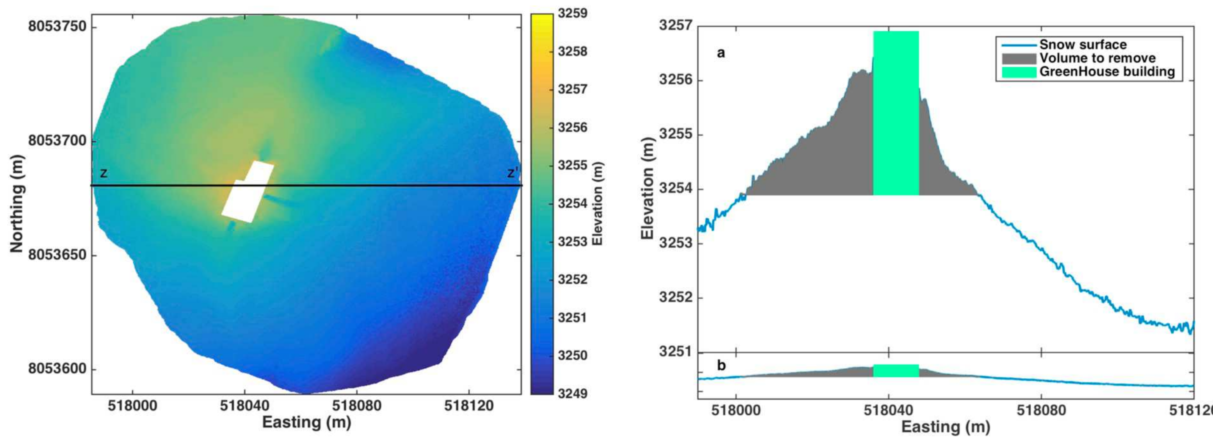

Fig. 6. Determining the volume of snow removed to clear the Greenhouse. Left: map-view showing elevations surrounding the Greenhouse (note the structure itself is masked), and cross section z-z'. Right, panel a) shows the snow surface along the transect z-z', the grade level of the original berm, and the volume of snow to be removed. Note vertical exaggeration. Panel b) shows the same view with no vertical exaggeration.

5.2. "Drifting-in" repeat time

Having determined the volume moved, and thus the effort required to clear any of these particular structures of drifted snow, we may wish to determine how long it may be until we have to repeat the task, as we will have exposed the building. Much work has been devoted to the task of modeling snowdrift around structures and terrain, with models of increasing physical complexity and fidelity (Section 2.1 and references therein). For the task at hand, we simply wish to determine an order-of-magnitude estimate of repeat time and annual drift volumes to be cleared, so we take a simpler, empirical approach, often used in the planning of polar camps (Haehnel and Weatherly, 2014). We use ten years of hourly wind data from the NOAA Earth System Research Laboratory site at Summit, in combination with simple drifting theory (Tabler, 1994), to estimate the time required to build up the full 'drifted in' volume.

Haehnel and Weatherly (2014) reported extensively on the estimation of drifting at polar camps, building upon the work of Tabler (1994). We use a formulation by Tabler (1994) of the regression equation from Mellor and Fellers (1986) to empirically derive the flux of drifting snow Q_{0-5} as a function of wind speed:

$$Q_{0-5} = U_{10}^{3.8}/233847 \qquad (1)$$

where U_{10} is the 10 m wind speed and Q_{0-5} is the snow transport in kg/s per meter of width across the wind.

Over an arbitrary-length fetch, 30% of the snow may be lost to sublimation (Tabler, 1994; Haehnel and Weatherly, 2014), so if we wish to determine the potential flux that could be deposited, we must consider only that flux that remains and so

$$Q_{dep} = 0.7 * Q_{0-5} \qquad (2)$$

where Q_{dep} is the mass flux of snow () deposited per unit cross-section relative to the wind.

To determine how often a building will drift in completely each year, we use hourly U_{10} observations from the NOAA meteorological suite at Summit, and integrate Eq. (2) over 12 months for ten years to determine the likely annual total Q_{dep}. We use for an example case the Greenhouse at Summit. Because the prevailing snow transport at Summit is not from a single direction by dominated by two orthogonal directions (Haehnel and Bigl, 2016), we use the average of the long and short axes of the building, which is roughly 17.5 m. The results of these calculations are summarized in Table 2. We use the existing 'drifted in' volume as a threshold at which point the building will be cleared.

Some important distinctions between actual snow clearing and our calculations must be acknowledged. First, once the building reaches the 'drifted in' state, further drifting is diminished or eliminated, so if the

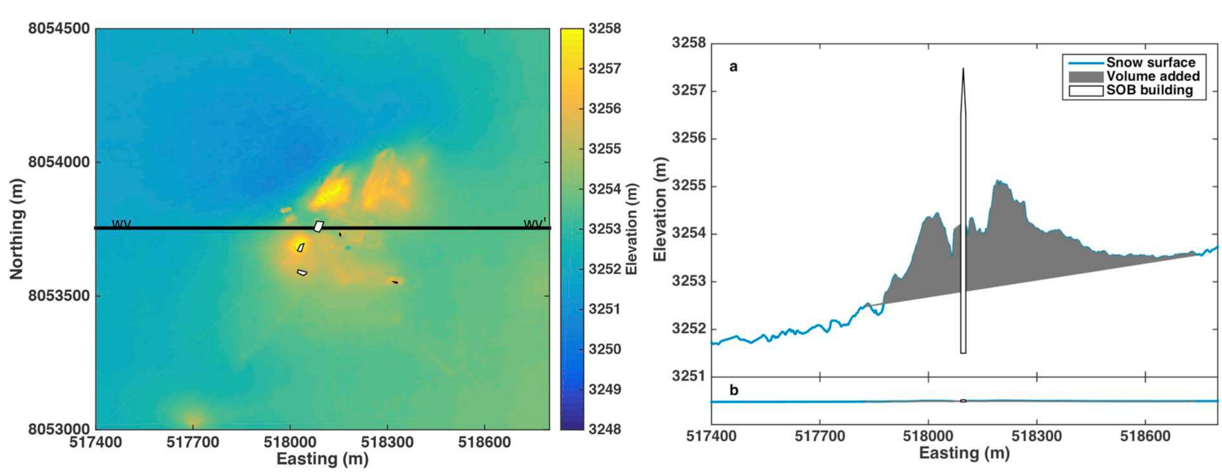

Fig. 7. Determining the volume of snow making up the Summit 'bulge'. Left: map-view showing elevations surrounding Summit (note the major structures are masked), and cross section wv-wv'. Right, panel a) shows the snow surface along the transect wv-wv', the regional grade level, and the volume of snow making up the bulge. Note vertical exaggeration. Panel b) shows the same view with no vertical exaggeration. DEM created by the Polar Geospatial Center from DigitalGlobe, Inc. imagery.

Table 1
Estimates of the volume of snow to be cleared at Summit, as a result of drifting around the buildings, and approximate number of equipment hours required, using the Caterpillar D6H LGP at Summit. Note that, given the variability in equipment efficiency, we round these hour results to two significant figures.

Structure	Volume (m^3)	Hours to clear
Greenhouse	4862 ± 444	69 ± 6
SOB "bowl"	4644 ± 272	66 ± 4
Deficit pile	39,168 ± 2036	560 ± 29
Summit "bulge"	583,018 ± 137,734	17,000 ± 2000

building were left in that state subsequent clearing of the building would be reduced. In reality this is not practical as entrances and windows must be cleared to provide safe egress from the building. Second, this analysis assumes that the building is fully drifted in before being cleared- in the summer this is also not usually the case, as the building is generally cleared well before it reaches the fully drifted-in state. Finally, through the winter months, it is impractical to clear the building each time it fully drifts in. This factor, coupled with the first distinction mentioned above, means that through the winter little additional snow drifts around the structure once an equilibrium drift is established. Significant effort must still be expended in this case to keep doors and windows clear for safe egress, and the snow removed from these spaces remains in the immediate vicinity of the building, requiring later transport (after winter). In agregate, the trade-offs between equilibrium drifting in winter and the more frequent, smaller-volume (and thus less efficient) snow removal in summer may cancel one another out in terms of equipment time and thus cost.

5.3. The true cost of buildings placed on snow

Combining the information from the first line in Table 2 with that from the first line in Table 1, we can determine the total operation time of the Caterpillar D6H LGP required to clear all of the snow from the Greenhouse in any given year. Using these numbers, the equipment time required to clear a volume of snow developed in Section 4, and an estimated D6H operating cost of $280 h^{-1} at Summit (Appendix A) we can calculate subsequent cost of snow removal from the Greenhouse in each year. We can generalize this to any building on the snow by determining the cost per meter of cross-section perpendicular to the prevailing wind. These costs are summarized in the last two lines of Table 2. As a historical note, the Greenhouse was installed in 1997, and

Table 2
Analysis of a ten-year meteorology record to determine drifting of the 'Greenhouse' building, and subsequent cost to clear. These numbers are based on the 17.5 m average cross section of the Greenhouse with respect to the snow transport direction. The 'annual cost per meter' is an estimate of the additional cost for snow removal for any new building placed on the snow. Note that due to the variability in estimating equipment cost per hour, we round cost estimates to two significant figures.

	Max	Min	Mean
Annual drift volume (m^3)	15,050	9138	11,702
Annual number of clearings	3.10	1.88	2.41
Annual cost of clearing	$53,000	$32,000	$41,000
Annual cost per meter	$3000	$1800	$2300

thus if we take the annual cost of clearing snow around it to be the average of $41,000, it follows that during its lifetime to date the greenhouse has cost a total of $820,000 for snow removal. Lift systems for polar buildings can be expensive as an up-front cost, but the hidden costs of removing snow from surface structures continue to add up over time.

6. Conclusions

Using UAV-based digital photogrammetry, we quantified the volume of snow drifted against, and cleared from, structures at Summit. We have shown that planners can use such UAV-based surveys to assist in effort estimates for snow-clearing operations in multiple geometries: a simple "pile" of snow, a building based below grade level, a building based on a berm above grade level, and a building elevated on legs above grade level. The building on legs generated no discernible drift, while the surface-based buildings accumulated significant drifting.

A typical structure placed on the snow at Summit accumulated 4862 ± 444 m^3 of snow, which we estimate would take 69 ± 6 h to clear with heavy equipment. We estimate the additional cost per year for one of these buildings, the Greenhouse, to be $41,000, and given its 20-year lifespan to date we estimate the total cost of clearing snow for the lifetime of the building to be $820,000. Elevated buildings are more expensive than their surface-based counterparts, but the money saved by placing a building on the surface may then be spent over time in the added costs of snow removal. In designing a station for long-term sustainability in a polar environment, an elevated building design is critical.

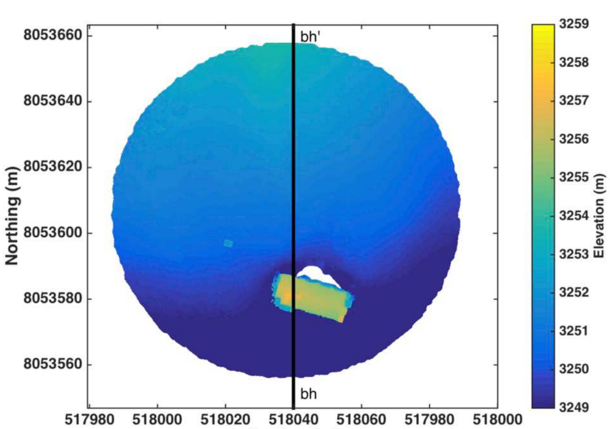

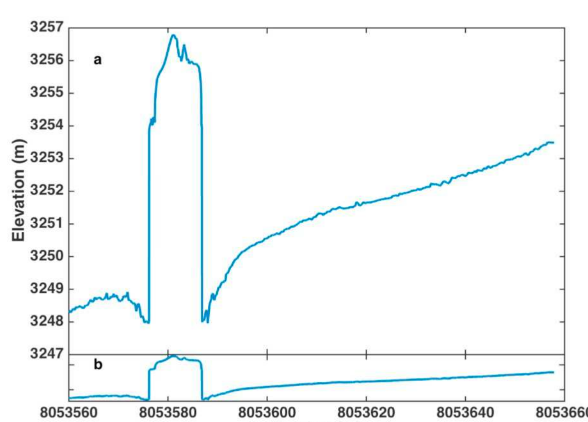

Fig. 8. DEM around the elevated 'Bighouse' at Summit, showing the impact of elevating structures. Left: map-view showing elevations surrounding the Bighouse, and cross section bh-bh'. The most likely area for drifting is centered, just downwind of the building. Right, panel a) shows the snow surface along the transect bh-bh', along with the profile of the building itself. Note vertical exaggeration. Though there is a gradual slope upwards towards the Greenhouse berm, little to no downwind drifting is evident. The depression caused by scouring beneath the building (as air speeds up through the constricted space under the building) can be readily seen. Panel b) shows the same view with no vertical exaggeration.

Acknowledgments

This project was supported by the National Science Foundation under grant NSF-ARC-1042358. We wish to thank Dr. Peter Gauer, Associate Editor, and three anonymous reviewers whose comments significantly improved the manuscript. Dr. Jonathan Chipman provided much helpful consultation on all things spatial. We thank Ben Toth for consultation on snow-moving productivity estimates. The large-scale satellite-derived DEM was provided by the Polar Geospatial Center under NSF OPP awards 1043681, 1559691 and 1542736. Meteorological data were provided by NOAA at http://www.esrl.noaa.gov.

Appendix A. Cost estimate: Caterpillar D6M

Calculating hourly ownership and operating costs of heavy equipment is an exercise in estimation (Caterpillar Inc, 2017). There are many factors influencing the actual costs, but we can arrive at an order-of-magnitude estimate using some published values and simple assumptions. Generally, the ownership cost is computed by amortizing the purchase price over the useful life of the equipment, in our case we assume a purchase price of $300,000, and a useful life of 10,000 h (averaging 20 h per week for 10 years). We neglect the common addition of loan interest and taxes in our case. The ownership cost is then $30 h $^{-1}$. The major operating costs include the amortized cost of preventive maintenance and inevitable repairs, the cost of fuel, and the operator's hourly wage. For preventive maintenance and repairs we consult the manufacturer's suggested values for operation in normal conditions, and to factor in the extreme environment we multiply the preventive maintenance by a factor of three, and repair by a factor of two, arriving at $7 h $^{-1}$ and $13 h $^{-1}$, respectively. The cost of fuel, once delivered to Summit, has been estimated to be $33 gal $^{-1}$ (Lever et al., 2016), and fuel consumption for "medium" working conditions is estimated to be 6 gal hr $^{-1}$ (Caterpillar Inc, 2017). Thus fuel cost calculates to $198 h $^{-1}$ which we round to $200 h $^{-1}$. The median hourly wage for a heavy equipment operator in the US is estimated to be $30 h $^{-1}$ (https://www1.salary.com/Heavy-Equipment-Operator-hourly-wages.html, accessed 22 Mar 2018). Total ownership and operating costs are thus $30 + $20 + $200 + $30 = $280.

References

Basnet, K., Muste, M., Constantinescu, G., Ho, H., Xu, H., 2016. Close range photogrammetry for dynamically tracking drifted snow deposition. Cold Reg. Sci. Technol. 121, 141–153.
Bernard, É., Friedt, J.-M., Tolle, F., Griselin, M., Marlin, C., Prokop, A., 2017. Investigating snowpack volumes and icing dynamics in the moraine of an arctic catchment using UAV photogrammetry. Photogramm. Rec. 32 (160), 497–512.
Bühler, Y., Adams, M.S., Bösch, R., Stoffel, A., 2016. Mapping snow depth in alpine terrain with unmanned aerial systems (uass): potential and limitations. Cryosphere 10 (3), 1075–1088.
Caterpillar Inc, 2017. Caterpillar Performance Handbook, 47th edition. Caterpillar, Peoria, Illinois, USA.
Cimoli, E., Marcer, M., Vandecrux, B., Bøggild, C.E., Williams, G., Simonsen, S.B., 2017. Application of low-cost uass and digital photogrammetry for high-resolution snow depth mapping in the arctic. Remote Sens. 9 (11), 1144.
Dibb, J., Fahnestock, M., 2004. Snow accumulation, surface height change, and firn densification at summit, Greenland: Insights from 2 years of in situ observation. J. Geophys. Res. 109 (D24), D24113.
Fonstad, M., Dietrich, J., Courville, B., Jensen, J., Carbonneau, P., 2012. Topographic Structure from Motion: A New Development in Photogrammetric Measurement. Earth Surface Processes and Landforms.
Gauer, P., 2001. Numerical modeling of blowing and drifting snow in alpine terrain. J. Glaciol. 47 (156), 97–110.
Haehnel, R.B., Bigl, M.F., 2016. Snow Drift Management: Summit Station Greenland. Tech. rep. Engineer Research and Development Center Hanover NH Cold Regions Research And Engineering Laboratory.
Haehnel, R., Weatherly, J., 2014. Antarctic Camps Snow Drift Management Handbook. Tech. rep.. DTIC Document.
Harder, P., Schirmer, M., Pomeroy, J., Helgason, W., 2016. Accuracy of snow depth estimation in mountain and prairie environments by an unmanned aerial vehicle. Cryosphere 10 (6), 2559.
Hugenholtz, C.H., Whitehead, K., Brown, O.W., Barchyn, T.E., Moorman, B.J., Leclair, A., Riddell, K., Hamilton, T., 2013. Geomorphological mapping with a small unmanned aircraft system (suas): feature detection and accuracy assessment of a photogrammetrically-derived digital terrain model. Geomorphology 194, 16–24.
Jaedicke, C., 2001. Acoustic snowdrift measurements: experiences from the flowcapt instrument. Cold Reg. Sci. Technol. 32 (1), 71–81.
Jaud, M., Passot, S., Le Bivic, R., Delacourt, C., Grandjean, P., Le Dantec, N., 2016. Assessing the accuracy of high resolution digital surface models computed by photoscan® and micmac® in sub-optimal survey conditions. Remote Sens. 8 (6), 465.
Kind, R., 1986. Snowdrifting: a review of modelling methods. Cold Reg. Sci. Technol. 12 (3), 217–228.
Koenderink, J.J., Van Doorn, A.J., 1991. Affine structure from motion. JOSA A 8 (2), 377–385.
Kwok, K., Kim, D., Smedley, D., Rohde, H., 1992. Snowdrift around buildings for antarctic environment. J. Wind Eng. Ind. Aerodyn. 44 (1), 2797–2808.
Lever, J.H., Phillips, G., Burnside, J., 2016. Economic Analysis of the Greenland Inland Traverse (Grit). Tech. rep. US Army Engineer Research and Development Center (ERDC) Hanover United States.
Liston, G.E., Haehnel, R.B., Sturm, M., Hiemstra, C.A., Berezovskaya, S., Tabler, R.D., 2007. Simulating complex snow distributions in windy environments using snowtran-3d. J. Glaciol. 53 (181), 241–256.
Mellor, M., Fellers, G., 1986. Concentration and Flux of Wind-Blown Snow. Tech. rep.. DTIC Document.
Miziński, B., Niedzielski, T., 2017. Fully-automated estimation of snow depth in near real time with the use of unmanned aerial vehicles without utilizing ground control points. Cold Reg. Sci. Technol. 138, 63–72.
Nolan, M., Larsen, C., Sturm, M., 2015. Mapping snow depth from manned aircraft on landscape scales at centimeter resolution using structure-from-motion photogrammetry. Cryosphere 9 (4), 1445–1463.
Piermattei, L., Carturan, L., Guarnieri, A., 2015. Use of terrestrial photogrammetry based on structure-from-motion for mass balance estimation of a small glacier in the italian alps. Earth Surf. Process. Landf. 40 (13), 1791–1802.
Pomeroy, J., Gray, D., 1990. Saltation of snow. Water Resour. Res. 26 (7), 1583–1594.
Prokop, A., Procter, E.S., 2016. A new methodology for planning snow drift fences in alpine terrain. Cold Reg. Sci. Technol. 132, 33–43.
Ryan, J., Hubbard, A., Box, J., Todd, J., Christoffersen, P., Carr, J., Holt, T., Snooke, N., 2015. Uav photogrammetry and structure from motion to assess calving dynamics at store glacier, a large outlet draining the Greenland ice sheet. Cryosphere 9 (1), 1–11.
Schneiderbauer, S., Prokop, A., 2011. The atmospheric snow-transport model: Snowdrift3d. J. Glaciol. 57 (203), 526–542.
Schön, P., Prokop, A., Vionnet, V., Guyomarc'h, G., Naaim-Bouvet, F., Heiser, M., 2015. Improving a terrain-based parameter for the assessment of snow depths with TLS data in the col du lac blanc area. Cold Reg. Sci. Technol. 114, 15–26.
Smedley, D., Kwok, K., Kim, D., 1993. Snowdrifting simulation around Davis station workshop, Antarctica. J. Wind Eng. Ind. Aerodyn. 50, 153–162.
Snavely, N., Seitz, S., Szeliski, R., 2008. Modeling the world from internet photo collections. Int. J. Comput. Vis. 80 (2), 189–210.
Tabler, R.D., 1994. Design Guidelines for the Control of Blowing and Drifting Snow. No. SHRP-H-381. Strategic Highway Research Program, National Research Council.
Tominaga, Y., Okaze, T., Mochida, A., 2011. Cfd modeling of snowdrift around a building: An overview of models and evaluation of a new approach. Build. Environ. 46 (4), 899–910.
Tominaga, Y., Okaze, T., Mochida, A., Sasaki, Y., Nemoto, M., Sato, T., 2013. Piv measurements of saltating snow particle velocity in a boundary layer developed in a wind tunnel. J. Vis. 16 (2), 95–98.
Vionnet, V., Martin, E., Masson, V., Guyomarc'h, G., Bouvet, F.N., Prokop, A., Durand, Y., Lac, C., 2014. Simulation of wind-induced snow transport and sublimation in alpine terrain using a fully coupled snowpack/atmosphere model. Cryosphere 8, 395.
Westoby, M., Brasington, J., Glasser, N., Hambrey, M., Reynolds, J., 2012. Structure-from-motion'photogrammetry: a low-cost, effective tool for geoscience applications. Geomorphology 179, 300–314.